

## Development of building height data from high-resolution SAR imagery and building footprint

F. Yamazaki

*Graduate School of Engineering, Chiba University, Chiba, Japan*

W. Liu

*Interdisciplinary Graduate School of Science and Engineering, Tokyo Institute of Technology, Yokohama, Japan;  
JSPS Research Fellow*

E. Mas & S. Koshimura

*International Research Institute of Disaster Science, Tohoku University, Sendai, Japan*

**ABSTRACT:** Extraction of man-made structures is one of essential issues in image processing of remotely sensed data. Due to remarkable improvements in radar sensors, high-resolution Synthetic Aperture Radar (SAR) images are available, providing detail ground surface information. In this study, a new method is developed to detect building heights automatically from a 2D GIS data and a single high-resolution TerraSAR-X (TSX) intensity image. A building in a TSX image shows layover from the actual position to the direction of the sensor due to the side-looking nature of SAR. Since the length of layover on a ground-range SAR image is proportional to the building height, it can be used to estimate the building height. To do this, we shift the building footprint obtained from 2D GIS data in the direction of the sensor. The proposed method is tested on a TSX image of Lima, Peru in the HighSpot mode with a resolution of about 1 m. The result showed a reasonable level of accuracy.

### 1 INSTRUCTIONS

In the last few years, imagery data from new high-resolution (HR) SAR sensors, e.g., Cosmo-SkyMed (CSM) and TerraSAR-X (TSX), have provided us with more detailed ground surface information. The features of an individual urban structure, especially its height, have become available from these SAR images. Although there have been several methods for obtaining height information from HR optical images, these methods were limited by the weather condition and daylight (Huang & Kwok, 2007; Hou *et al.*, 2011). Several methods related to height detection from HR SAR images have been proposed, and they can be divided into three categories.

The first category is interferometric (InSAR) analysis. Bolter & Leberl (2000) extracted buildings and their heights from multiple-view InSAR datasets. Thiel *et al.* (2007) used two approaches to detect buildings of different sizes from multi-aspect HR InSAR datasets. Building features were extracted independently for each direction from the amplitude and phase information in the InSAR data. These methods, however, require at least two SAR images in different flight angles. The second category is based on a direct electromagnetic backscattering model. Franceschetti *et al.* (2002) proposed a method for extracting the

building height information based on a radiometric analysis of the double-bounce contribution. They tested this method upon an airborne SAR sensor image (2007), and Liu *et al.* (2009) applied the method to a TSX image of Shanghai, China. This method requires prior knowledge of the material and surface roughness properties of the background, and it cannot be used in different areas. The third category is based on the geometrical characteristics of layover and radar-shadow areas. Xu & Jin (2005) proposed a method for the automatic reconstruction of building objects from multi-aspect very HR SAR data. Brunner & Lemoine (2010) estimated building heights by matching simulated SAR images with a real image containing buildings of various heights. However, these methods were complicated and time consuming.

The building height information is often used in earthquake and tsunami damage assessment. In this regard, the present authors are involved in the earthquake and tsunami disaster mitigation program in Peru (Yamazaki & Zavala, 2013), sponsored by Japan Science and Technology Agency (JST) and Japan International Cooperation Agency (JICA) in the framework of “the Science and Technology Research Partnership for Sustainable Development (SATREPS)”. To assess tsunami risk in Lima, Peru, Mas *et al.* (2013) simulated tsunami inundation and human evacuation behavior.

The 3D modeling of buildings is necessary for this objective, and hence the use of high-resolution SAR imagery is investigated herein.

In this study, a simple method is proposed for detecting the heights of individual buildings by estimating their layover lengths from a single HR SAR image. The footprint of a single building taken from 2D GIS data is needed to create a template on a SAR image. The template is then shifted to the direction of the sensor step by step. In each step, the inside area of the template is calculated to distinguish the boundaries of layover. This method was applied to a TSX image of La Punta district, Lima, Peru. In addition, the visual interpretation of building heights from a WorldView-2 (WV-2) image was introduced as a reference to verify the accuracy of the proposed method.

## 2 THE STUDY AREA AND IMAGE DATA

The study area focuses on a coastal area of Lima, Peru, as shown in Figure 1(a). A TSX image taken on February 18, 2008, shown in Figure 1(b), was used to detect building heights. The image was taken by the VV polarization in the ascending path. Since the image was taken in the HighSpot Mode (HS), the azimuth resolution was about 1.10 m and the ground range resolution was about 1.00 m. The image was recorded as a single-look slant-range complex (SSC) product. The proposed method was applied on the La Punta district, which is shown in Figure 1(b) by the yellow frame. Since this area was frequently affected by tsunamis, a highly accuracy tsunami run-up simulation with accurate building models will help for disaster mitigation.

Several pre-processing steps were carried out on the image prior to the detection of building heights. First, the TSX image was transformed into a geocoded ground range amplitude image using SARscape software. Since the digital elevation model (DEM), converted from topography data based on contour lines, was used for geocoding as shown in Figure 1(c). It was confirmed that the topography of this area is flat with low elevation, which is easily affected by tsunamis. Then the processed TSX image was resampled as 0.5 m/pixel. Next the image was transformed into a Sigma Naught ( $\sigma^0$ ) value, which represents the radar reflectivity per unit area in the ground range, following the radiometric calibration process. An enhanced Lee filter (Lopes *et al.*, 1990), one of the most commonly used adaptive filters, was used to reduce the speckle noise in the original SAR image, which makes the radiometric and textural aspects less efficient. To prevent the loss of the information included in the intensity images, the window size of the filter was set as small as possible, i.e.  $3 \times 3$  pixels (about  $1.5 \text{ m} \times 1.5 \text{ m}$ ). The TSX image after all the pre-processing steps is shown in Figure 2(a).

To estimate the building height from TSX images, outline data of buildings are requested. A 2D GIS map including lot boundaries was used in this study as the

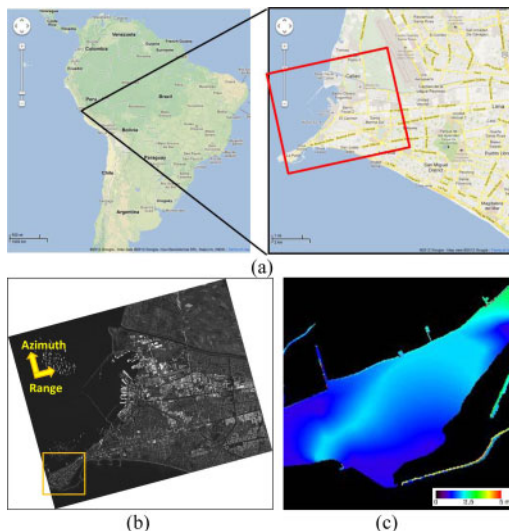


Figure 1. Study area along the Pacific-coast of Lima, Peru (a); the TSX image taken on Feb. 18, 2008 (b); the DEM converted from geometry data based on contour lines (c).

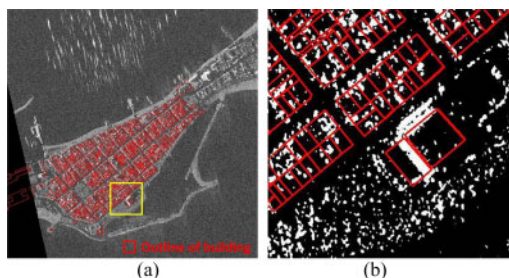


Figure 2. Outline of buildings overlapped on the pre-processed TSX image (a), and a close-up in the yellow frame of the binary SAR image (b).

footprints of buildings. The outlines are shown in Figure 2(a) by red lines, overlapping on the pre-processed TSX image. Although the number of stories for each building is included in the GIS data, more accurate building height information is useful for a tsunami evacuation analysis. From Figure 2(a), most of the outlines seem to be matched with the location of buildings in the TSX image.

## 3 METHOD OF HEIGHT DETECTION

Due to the side-looking nature of SAR, a building in a TSX image shows a layover from the actual position, to the direction of the sensor, as shown in Figure 3. The layover is proportional to the building height, as expressed in Equation (1).

$$L = H / \tan \theta \quad (1)$$

where  $\theta$  is the incident angle of radar in the TSX image.

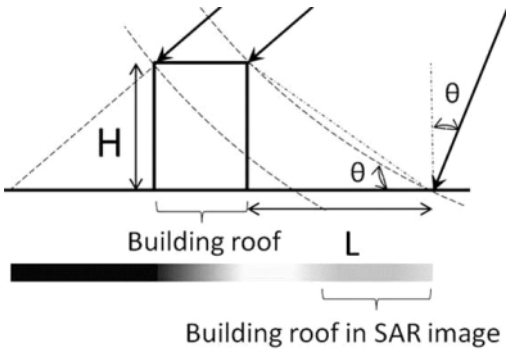


Figure 3. Schematic plot of the location of a building in a SAR image.

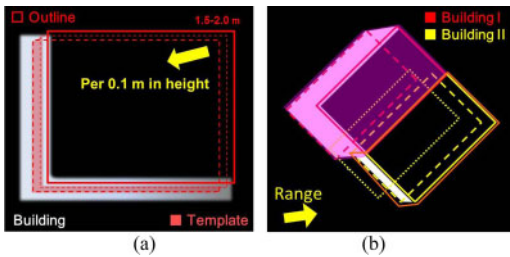


Figure 4. Simulation of the template for layover search (a), and boundary definition for two connected buildings with different heights (b).

From Figure 2(a), it is obvious that the high backscatter areas due to building walls were away from the building footprint. If the length of the layover along the sensor direction is detected, the height of the building can be calculated using Equation (1).

To detect the layover length, a template was created based on the building outline and was then shifted in the direction of the SAR sensor (southwest). Since a typical building is usually higher than 2 m, 2 m was set as the initial height for searching a layover area. Due to the  $53.91^\circ$  incidence angle and the  $347.65^\circ$  path angle (clockwise from the north), a 2-m building shows a 2.36-m layover to the west and a 0.41-m layover to the south. The width of the layover increases 0.73 m to the west and 0.16 m to the south, for a 1-m increase in the building height.

Considering the resolution and pixel size of the TSX image, the width of the template was set as a 0.5-m building height. Thus, the initial template for the layover of a wall with a height between 2.0 m and 2.5 m was created, as shown in the yellow block in Figure 4(a). Since most of the layover occurs on a street area, the area within the building outline was removed from the template. Thus, the shape of the template depends on the size of the building and on the surrounding conditions.

In the theory, a building of  $5 \times 5 \text{ m}^2$  would have a template of about  $2.2 \text{ m}^2$ . However, in the case of buildings standing in a row, the layover area is seen only in one direction and is relatively small. To confirm

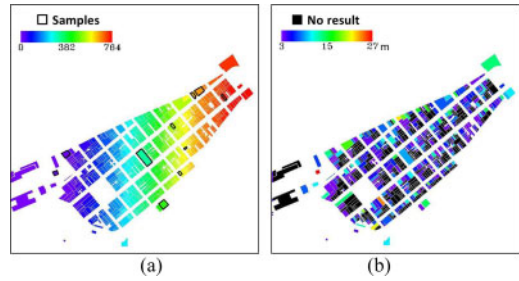


Figure 5. ID numbers were assigned for 764 buildings according to their distance from the SAR sensor (a) and the detected heights for 398 buildings (b).

that there is enough information within a template, a single template should be larger than  $1.0 \text{ m}^2$ . If there is not a large enough initial template, as in the case that it is enclosed by other buildings, layover search will not begin. Next the created template is shifted in the direction of the sensor step by step, by increasing the building height at an interval of 0.1 m. To improve the accuracy of the height detection, the area in the TSX image surrounding a building was resampled to 0.1 m by cubic convolution, which is 1/5 of the initial pixel size.

To estimate the boundary of layover, two methods were used to define the threshold values. The first method was used to define the threshold value for the backscattering intensity. The average value of the backscatter in the TSX image within the template is calculated. When it is lower than the threshold value, the template is classified as a street and the shifting is stopped. However, this method shows errors when there is an outstanding bright or dark object within the template.

The second method was used to define the threshold value for the areal percentage. In this method, the TSX image is first divided into a binary image using one threshold value. High backscatter areas such as corner reflections and the layover of walls are transformed as 1, whereas low backscatter areas such as radar shadows and roads are 0. Next, the percentage of high backscatter areas within a template is calculated. When the percentage is lower than a threshold value, the template is classified as a street. In this study, the latter method was selected. The TSX image was divided by the average backscattering intensity of the entire image, which is  $-10.5 \text{ dB}$ . A part of a binary image is shown in Figure 2(b).

Next, the threshold value for the areal percentage was investigated for 10 buildings as an example. The sample buildings are shown in Figure 5(a) by bold black lines. According to the GIS data, the maximum building story is 9 in this area. Thus, the maximum building height was set as 30 m, which means the maximum searching distance for layover is 21.50 m to the west and 4.71 m to the south. The percentage value within a template for each building was recorded as shifting the template, which is shown in Figure 6(a). Then a filter was applied to smooth these

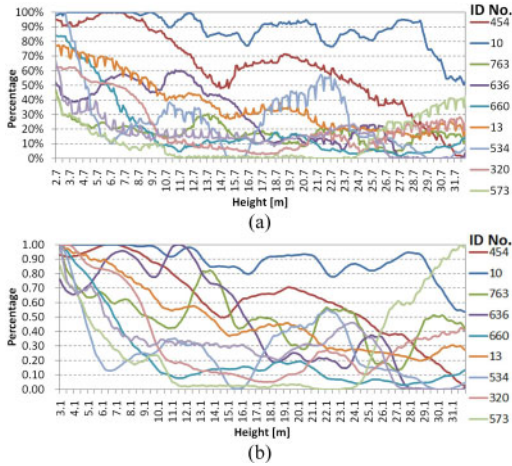


Figure 6. Change of percentage values for ten sample buildings during the template shifting from 2.5 m to 33.0 m (a); the percentage values after smoothing by averaging 10 consecutive values and then standardized by their maximum (b).

percentage values by averaging 10 consecutive values. The smoothed percentage values were standardized by their maximum values respectively, as shown in Figure 6(b). It could be confirmed that the percentage value in a template is highest at the beginning and it goes lower as shifting the template. However, when the template is shifted over another building, the percentage value goes higher again. Thus, once the percentage value is lower than a threshold value, the last location was used to estimate the height in this study. According to the number of stories in the GIS data, a reference height was obtained by multiplying the number of stories with 3 m, which is regarded as the average height of one story. The percentage values for these samples on the reference heights were obtained and averaged as the final threshold value, which is 51% in this area. Thus, once the smoothed standardized percentage value reaches less than 51%, the last location of layover is considered as the boundary.

When there are two buildings of different heights with no space between them, their layover areas, which have different lengths, are also connected as shown in Figure 4(b). If two templates of buildings shift at the same time, the template for Building II, indicated by a yellow dotted line, will search both layover areas. Then, the height of Building II cannot be detected correctly. Thus, the order of the layover search is important. In this study, to confirm that template shifting was performed in the correct order, an ID number was assigned to each building. A smaller ID number was assigned to buildings located closer to the direction of the sensor. Next, the template was created and shifted in the order of ascending ID numbers. Once a layover area has been searched, it was masked and will not be searched again. As seen in the case of Figure 4 (b), the layover area of Building I was searched first and the final boundary is indicated by a red dashed line. Next, the area of Building I and its layover area

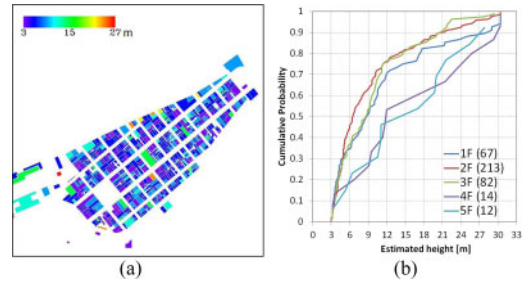


Figure 7. Reference building heights obtained by multiplying the number of stories with 3 m (a); comparison of the detected heights with the number of stories in the GIS data on the cumulative distribution plot (b).

were masked when searching for Building II. Finally, the boundary of Building II was detected correctly; this boundary is indicated by a yellow dashed line.

#### 4 DETECTED RESULTS AND VERIFICATION

The proposed method was applied to the target area shown in Figure 2(a). According to the GIS data, 764 buildings exist there. They were then numbered based on their distances from the SAR sensor, as shown in Figure 5(a). The layover areas were searched in the order of their ID numbers, and their lengths were used to calculate the building heights. Since the maximum height from the layover search was set as 30 m, which is equal to the height of a ten-story building (the height of one story is counted as 3 m). The heights of 398 buildings were detected successfully, and the results are shown in a rainbow array of colors in Figure 5(b). Some buildings could not be detected because of their surrounding conditions. Most of these buildings were located behind other buildings, so there was no space for the creation of a template.

A reference height was obtained according to the number of stories in the GIS data, as shown in Figure 7(a). Comparing Figure 5(b) and Figure 7(a), we can observe that several buildings are shown in a similar color, which means they have similar heights. Since the real heights of buildings were unknown, it is difficult to verify the accuracy of proposed method. Thus, two methods were used in this study to verify the estimated results. The first one is the comparison with the GIS data, and the second one is visual interpretation of a high-resolution optical image from WorldView-2 (WV-2) satellite.

##### 4.1 Comparison with the GIS data

A comparison between the estimated height and the number of stories in the GIS data was carried out. The estimated heights with the same number of stories were grouped as one. Then the heights in each group were relined by the ascending order. The cumulative probability of the estimated height for each storied building was calculated and shown in Figure 7(b). The height

Table 1. Number of estimated buildings and their median heights in each story class.

Number of stories	1F	2F	3F	4F	5F
Number of buildings	67	213	82	14	12
Median height [m]	8.7	6.5	8.7	12.0	17.0

with the probability of 0.5 is the median height for this group. Considering the number of buildings in each group, the cumulative distributions were drawn for one to five-storied buildings only.

From Figure 7(b), it can be confirmed that the median values of the estimated heights go higher as the number of stories increases. However, the median height for one-storied buildings was 8.7 m, which equals to the average height for three-storied buildings. The median heights for one to five-storied buildings are shown in Table 1. Except for the one-storied buildings, the median values of the estimated heights were similar to the values obtained by multiplying the number of stories with 3 m.

The errors for one-storied buildings were caused in the layover search step. Since the layover search starts from 2.5 m, the layover area for a one-storied building is very small. After the smoothing and standardizing process for recording percentage values from 2.5 m to 30.0 m, the value of layover becomes smaller than the real one. Therefore, it is difficult to distinguish the layover of one-storied buildings from the street area. However, the proposed method is possible to estimate the height of individual buildings equal to or more than two-storied. Another basic reason for the errors is the building footprint data. Since the outline of each lot was used as a building footprint in this study, the difference between them caused errors in the layover search step. The accuracy of our proposed method can be improved by introducing more accurate footprint data.

#### 4.2 Comparison with the WorldView-2 image

A World-View-2 (WV-2) image taken on December 27, 2010 was introduced to verify the accuracy of the proposed method, as shown in Figure 8(a). The ground resolution for its panchromatic image is 0.50 m, which is the same as the pixel size of the pre-processed TSX image. According to Huang & Kwok (2007), the height of an individual building can be estimated by Equation (2) from a HR optical satellite image.

$$h = \frac{L}{\sqrt{\frac{1}{\tan^2 \lambda'} + \frac{1}{\tan^2 \lambda} - \frac{2 \cos(\alpha - \alpha')}{\tan \lambda' \cdot \tan \lambda}}} \quad (2)$$

where  $L$  is the distance between the top point of the building and the same point of its shadow in the satellite image; the azimuth and elevation angle of the

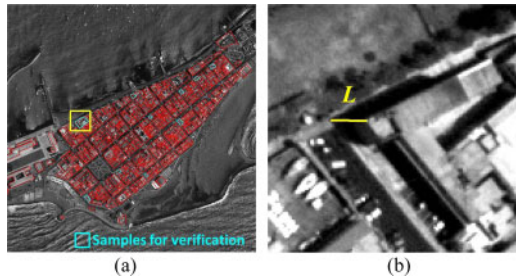


Figure 8. Panchromatic WorldView-2 image taken on Dec. 18, 27, 2010 (a); a close-up of the yellow frame to estimate the height by visual interpretation (b).

Table 2. Comparison of the estimated height from the TSX image and that from the WorldView-2 image by visual interpretation. [m]

ID number	TSX	WV-2	Difference
51	7.30	7.4	0.10
87	7.30	5.2	-2.10
226	8.62	5.9	-2.72
304	9.95	9.9	-0.05
381	6.96	4.4	-2.56
406	13.93	17.7	3.77
585	11.27	10.1	-1.17
592	5.97	6.1	0.13
667	10.61	8.6	-2.01
709	21.89	22.1	0.21

satellite are  $\alpha$  and  $\lambda$ , respectively; and the azimuth and elevation angles of the sun are  $\alpha'$  and  $\lambda'$ , respectively.

Ten buildings except for the samples used for defining the threshold value were selected, as shown in Figure 8(a) by cyan lines. The lengths of  $L$  for these buildings were measured from the WV-2 image manually to estimate the height. An example is shown in Figure 8(b). According to the header file of the WV-2 image, the azimuth angle of the sun is  $103.3^\circ$  and its elevation angle is  $65.2^\circ$ . The azimuth angle for the satellite is  $255.7^\circ$  while the elevation angle is  $72.6^\circ$ . Since the measured distance of  $L$  in Figure 8(b) is 20 pixels, the height of this building could be obtained as about 13.3 m by Equation (2). The height estimated from the TSX image by our method is 17.7 m. The heights for the ten buildings were obtained as shown in Table 2. A comparison of the detected heights and the reference heights is shown in Figure 9.

From the figure, it could be confirmed that the estimated heights from the TSX image are very close to the result of visual interpretation from the WV-2 image. The maximum difference between the estimated height from layover and the result from visual interpretation was 3.77 m. Most of the differences were less than 3 m, which is the average height of one story. The average value of the differences is  $-0.64$  m while the Root Mean Square (RMS) error is 1.95 m, which is also less than the average height of one story.

Since the assignments of top points for both the building and its shadow are needed, the heights of

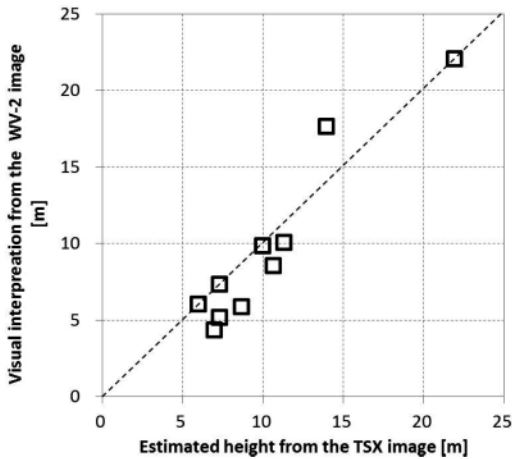


Figure 9. Comparison of the estimated building heights versus the visual interpretation results from the WV-2 image.

many buildings could not be measured by visual interpretation. In addition, visual interpretation requires time and efforts. On the contrary, our proposed method can estimate building heights automatically from a single TSX image, and its result is similar to that of visual interpretation. Thus, it is more efficient than visual interpretation from HR optical images.

## 5 CONCLUSIONS

In risk assessments for natural disasters, e.g. earthquakes, tsunamis and floods, exposure data such as building inventory are necessary together with hazard information and vulnerability functions. Three-dimensional building information is important, especially for tsunami damage assessment and evacuation planning. But building height data are not so easy to prepare.

In this study, a method to detect the height of an individual building from a high-resolution TerraSAR-X image was proposed by measuring the length of layover. The method was tested using a 1-m resolution SAR image of Lima, Peru. The footprints of 764 buildings from GIS data were overlapped on the TSX image to detect the building heights. As a result, the heights of 398 buildings were detected successfully. The estimated building heights were compared with the number of stories stored in the GIS data and the visual interpretation result from a WorldView-2 optical satellite image. By plotting the cumulative distribution of the estimated heights of buildings, the median height for buildings was similar to 3 times of the story number. Since the normal average height for one story is about 3 m, our method is possible to estimate the building height rather accurately.

Ten buildings were selected as samples to verify the accuracy of the results. Their heights were measured from the WV-2 image manually. Comparing the estimated results from the TSX image with those from

visual interpretation, the average difference between them for the ten samples was  $-0.64$  and the RMS error was 1.95 m, which is less than the height of a single story.

However, there still exist some errors in the estimated results. The accuracy of the proposed method depends on the surrounding conditions of the target building and the shape of building footprints. Since the outlines of lots were used instead of that of a building, many miss-matching occurred in the layover search step. However, the results show that our method is generally useful for estimating building heights.

In the future, the method will be tested on more high-resolution SAR images of different locations to verify its accuracy and to examine its limitation. Our method is conveniently used for the creation of 3D city model, which is employed in tsunami inundation and human evacuation simulation.

## REFERENCES

- Bolter, R. & Leberl, F., 2000. Detection and reconstruction of human scale features from high resolution interferometric SAR data, In *Proc. 15th Int. Conf. Pattern Recognition* 4:91–294.
- Brunner, D. & Lemoine, G., 2010. Building height retrieval from VHR SAR imagery based on an iterative simulation and matching technique, *IEEE Trans. Geoscience and Remote Sensing* 48(3): 1487–1504.
- Franceschetti, G., Iodice, A. & Riccio, D. 2002. A canonical problem in electromagnetic backscattering from buildings, *IEEE Trans. Geoscience and Remote Sensing* 40(8): 1787–1801.
- Franceschetti, G., Guida, R., Iodice, A., Riccio, D. & Ruello, G., 2007. Building feature extraction via a deterministic approach: Application to real high resolution SAR images, *Proc. IEEE IGARSS*: 2681–2684.
- Hou, X., Qi, M., Li, D., Lv, G., Wang, Y., 2011. The model of extracting the height of buildings by shadow in image, *Proc. ICCSNT* 4: 2150–2153.
- Huang, X. & Kwok, L. K., 2007. 3D building reconstruction and visualization for single high resolution satellite image, *Proc. IEEE IGARSS*: 5009–5012.
- Liu, K., Balz, T. & Liao, M., 2009. Building height determination by TerraSAR-X backscatter analysis in dense urban areas, *Proc. 2009 Asian Conference on Remote Sensing*.
- Lopes, A., Touzi, R. & Nezry, E., 1990. Adaptive Speckle Filters and Scene Heterogeneity, *IEEE Trans. Geoscience and Remote Sensing* 28(6): 992–1000.
- Mas, E., Adriano, B., Koshimura, S., 2013. An integrated simulation of tsunami hazard and human evacuation in La Punta, Peru, *Journal of Disaster Research* 8(2): 285–295.
- Thiele, A., Cadario, E., Schulz, K., Thoennessen, U. & Soergel, U., 2007. Building recognition from multi-aspect high-resolution InSAR data in urban areas, *IEEE Trans. Geoscience and Remote Sensing* 45(11): 495–505.
- Xu, F. & Jin, Y.-Q., 2005. Deorientation theory of polarimetric scattering targets and application to terrain surface classification, *IEEE Trans. Geoscience and Remote Sensing* 43(10): 2351–2364.
- Yamazaki, F. & Zavala, C., 2013. SATREPS Project on Enhancement of Earthquake and Tsunami Disaster Mitigation Technology in Peru, *Journal of Disaster Research* 8(2): 224–234.